

Insight into influence of thermodynamic coefficients on transient negative capacitance in Zr-doped HfO_2 ferroelectric capacitors

Yuan-Yuan Zhang(张元元), Xiao-Qing Sun(孙晓清), Jun-Shuai Chai(柴俊帅), Hao Xu(徐昊), Xue-Li Ma(马雪丽), Jin-Juan Xiang(项金娟), Kai Han(韩锴), Xiao-Lei Wang(王晓磊), and Wen-Wu Wang(王文武)

Citation: Chin. Phys. B, 2021, 30 (**12**): 127701. DOI: 10.1088/1674-1056/ac01c4
Journal homepage: http://cpb.iphy.ac.cn; http://iopscience.iop.org/cpb

What follows is a list of articles you may be interested in

Irradiation behavior and recovery effect of ferroelectric properties of PZT thin films

Yu Zhao(赵瑜), Wen-Yue Zhao(赵文悦), Dan-Dan Ju(琚丹丹), Yue-Yue Yao(姚月月), Hao Wang(王豪), Cheng-Yue Sun(孙承月), Ya-Zhou Peng(彭亚洲), Yi-Yong Wu(吴宜勇), and Wei-Dong Fei(费维栋)
Chin. Phys. B, 2021, 30 (**10**): 107702. DOI: 10.1088/1674-1056/ac0dad

Effects of Ni substitution on multiferroic properties in $Bi_5FeTi_3O_{15}$ ceramics

Hui Sun(孙慧), Jiaying Niu(钮佳颖), Haiying Cheng(成海英), Yuxi Lu(卢玉溪), Zirou Xu(徐紫柔), Lei Zhang(张磊), and Xiaobing Chen(陈小兵)
Chin. Phys. B, 2021, 30 (**10**): 107701. DOI: 10.1088/1674-1056/ac1b92

Sr-doping effects on conductivity, charge transport, and ferroelectricity of $Ba_{0.7}La_{0.3}TiO_3$ epitaxial thin films

Qiang Li(李强), Dao Wang(王岛), Yan Zhang(张岩), Yu-Shan Li(李育珊), Ai-Hua Zhang(张爱华), Rui-Qiang Tao(陶瑞强), Zhen Fan(樊贞), Min Zeng(曾敏), Guo-Fu Zhou(周国富), Xu-Bing Lu(陆旭兵), and Jun-Ming Liu(刘俊明)
Chin. Phys. B, 2021, 30 (**2**): 027701. DOI: 10.1088/1674-1056/abc15a

Recent advances, perspectives, and challenges inferroelectric synapses

Bo-Bo Tian(田博博), Ni Zhong(钟妮), Chun-Gang Duan(段纯刚)
Chin. Phys. B, 2020, 29 (**9**): 097701. DOI: 10.1088/1674-1056/aba603

Electrocaloric effect enhanced thermal conduction of a multilayer ceramic structure

Hongbo Liu(刘宏波)
Chin. Phys. B, 2020, 29 (**8**): 087701. DOI: 10.1088/1674-1056/ab942f

---

Insight into influence of thermodynamic coefficients on transient negative capacitance in Zr-doped HfO_2 ferroelectric capacitors*

Yuan-Yuan Zhang(张元元)[1,2], Xiao-Qing Sun(孙晓清)[1,2], Jun-Shuai Chai(柴俊帅)[1,2,†], Hao Xu(徐昊)[1,2], Xue-Li Ma(马雪丽)[1,2], Jin-Juan Xiang(项金娟)[1,2], Kai Han(韩锴)[3], Xiao-Lei Wang(王晓磊)[1,2,‡], and Wen-Wu Wang(王文武)[1,2]

[1] *Key Laboratory of Microelectronics & Integrated Technology, Institute of Microelectronics, Chinese Academy of Sciences, Beijing* 100029, *China*
[2] *College of Microelectronics, University of Chinese Academy of Sciences, Beijing* 100049, *China*
[3] *Department of Physics and Electronic Science, Weifang University, Weifang* 261061, *China*

(Received 9 May 2021; revised manuscript received 13 May 2021; accepted manuscript online 16 May 2021)

We study the influence of the thermodynamic coefficients on transient negative capacitance for the Zr-doped HfO_2 (HZO) ferroelectric capacitors by the theoretical simulation based on the Landau–Khalatnikov (L-K) theory and experimental measurement of electrical properties in the resistor-ferroelectric capacitor (*R*-FEC) circuit. Our results show that the thermodynamic coefficients α, β and γ also play a key role for the transient NC effect besides the viscosity coefficient and series resistor. Moreover, the smaller coefficients α and β, the more significant the transient NC effect. In addition, we also find that the thermodynamic process of transient NC does not obey the generally accepted viewpoint of Gibbs free energy minimization.

Keywords: transient negative capacitance (NC), ferroelectric, hafnium-zirconium oxide

PACS: 77.80.–e, 85.50.–n, 77.84.–s, 85.30.Tv **DOI:** 10.1088/1674-1056/ac01c4

1. Introduction

The power consumption of microprocessors has significantly increased with the improvement of computing power, due to the ongoing pursuit of Moore's law.[1–4] Reducing the power consumption of devices is thus a key challenge in contemporary information industry.[5–8] However, a fundamental thermodynamic limit of 60 $mV{\cdot}dec^{-1}$ at room temperature, which is known as Boltzmann limit, impedes the reducing of power consumption for conventional device.[9,10] In order to overcome this limit, the steep subthreshold swing devices are required.

Negative capacitance field effect transistor[11–22] (NCFET) is a promising steep subthreshold swing device, which is expected to work at extremely low supply voltages.[23,24] It becomes thus a potential candidate for the next generation of low power transistors. So far, there are two types of NC (steady-state NC[25,26] and transient NC[27–33]) that have been extensively reported. The steady-state NC has been indirectly demonstrated by total capacitance enhancement in ferroelectric-dielectric (FE-DE) superlattices and heterostructures.[34–37] It can be understood from the viewpoint of energy: the negative curvature region of ferroelectric Gibbs free energy landscape is stabilized by the superposition of ferroelectric and dielectric energy landscapes. However, the existence of the steady-state NC has a great controversy in recent years.[38–40] For the transient NC, it has been experimentally observed in the series circuit of resistor and ferroelectric capacitors (*R*-FEC)[27–31] and theoretically understood by the Landau–Ginzburg–Devonshire (L-G-D) theory.[41–44] The transient NC is caused by the mismatch between the ferroelectric polarization switching rate and the circuit current.[45–47] This means that transient NC cannot exist stably, and can only appear in the process of ferroelectric polarization switching. The previous studies have reported that the transient NC is affect by external resistors and viscosity coefficients.[45,48] However, the related studies on the influences of more intrinsic ferroelectric material parameters and extrinsic factors in the *R*-FEC circuit for transient NC are lacked and need to be clarified.

In this work, using the theoretical simulation based on the Landau–Khalatnikov (L-K) theory and experimental measurement of electrical properties, we systematically investigate the influence of thermodynamic coefficients on transient NC for the Zr-doped HfO_2 (HZO) ferroelectric capacitors in the *R*-FEC circuit. Our results show that transient NC is not only related to series resistor and viscosity coefficient, but also thermodynamic coefficients α, β, and γ. Moreover, we find that the smaller the α and β, the more conducive to the appearance of the transient NC. In addition, we also find that the generally accepted viewpoint of Gibbs free energy minimization is not applicable to explain the transient NC effect of ferroelectric capacitors.

*Project supported by the National Key Project of Science and Technology of China (Grant No. 2017ZX02315001-002).
†Corresponding author. E-mail: chaijunshuai@ime.ac.cn
‡Corresponding author. E-mail: wangxiaolei@ime.ac.cn
© 2021 Chinese Physical Society and IOP Publishing Ltd

2. Experimental details and theoretical model

2.1. Experimental details

The metal–ferroelectric–metal (MFM) capacitors were fabricated with the top and bottom electrodes, as shown in Fig. 1. Si substrate was cleaned by standard wet clean. Then, the bottom electrode (TiN), the 10-nm-thick Zr-doped HfO_2 (HZO) thin film and top electrode (TiN and W) were deposited by atomic layer deposition[49,50] (ALD) in turn. The HZO thin films were crystallized in N_2 ambient and rapid thermal anneal (RTA) system of 550–650 °C. The composition of the HZO thin film was changed by controlling the deposition ratio of HfO_2 and ZrO_2 to realize the adjustment of ferroelectric intrinsic parameters (thermodynamic coefficients α, β and γ, etc) and form the ferroelectric capacitors with different Hf:Zr ratios. The range of ZrO_2 content is from 10% to 90%, as listed in Table 1.

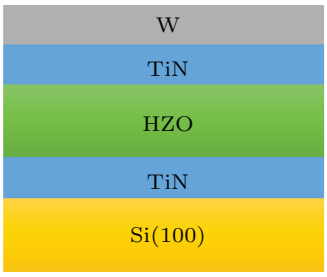


Fig. 1. The schematic of TiN/HZO/TiN ferroelectric capacitor.

Table 1. HZO thin films with different ZrO_2 contents.

Sample	1	2	3	4	5	6	7
Hf:Zr	0.9:0.1	0.75:0.25	0.6:0.4	0.5:0.5	0.4:0.6	0.25:0.75	0.1:0.9

2.2. Theoretical model

In order to investigate the transient NC effect of the ferroelectric HZO capacitors, we adopt the numerical simulation method. For the ferroelectric material, we use the L-K model,[51] which means that polarization switching obeys the energy minimization. In this model, the relationship of P–V_{FE} can be expressed as

$$\rho\frac{dP}{dt} = -2\alpha P - 4\beta P^3 - 6\gamma P^5 + \frac{V_{FE}}{d_{FE}}, \tag{1}$$

where α, β and γ represent the thermodynamic expansion coefficients. ρ represents the viscosity coefficient and reflects the delay of polarization P. E_{FE} represents the electric field across the ferroelectric material, and d_{FE} represents the ferroelectric material thickness. The L-K model describes the dynamic process of polarization with the time.

In R-FEC circuit (see Fig. 2), the Kirchhoff's rules can be written as

$$RA\frac{dD}{dt} = V_S - V_{FE}, \tag{2}$$

where R represents the external resistance, A represents the ferroelectric material area, and V_S represents the source voltage. The expression of electric displacement field D is

$$D = P + \varepsilon_0\frac{V_{FE}}{d_{FE}}. \tag{3}$$

Kirchhoff's rule describes the dynamic process of free charge with time. Combing with Eqs. (1)–(3), we can obtain the dynamic response of transient NC.

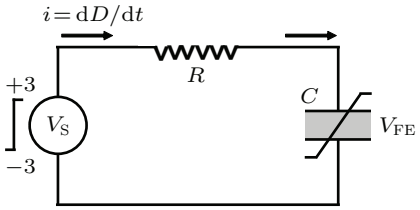


Fig. 2. The schematic of an R-FEC circuit. C denotes the ferroelectric capacitor and R represents the external resistor. V_{FE} and V_S represent the voltage across the FE and the applied voltage, respectively.

3. Results and discussion

3.1. Influence of thermodynamic coefficients on transient NC based on the theoretical derivation

We first investigate the affect factors of transient NC by rigorous theoretical derivation. Taking a derivation of Eq. (3) to time t yields

$$\frac{dV_{FE}}{dt} = \frac{d_{FE}}{\varepsilon_0}\left(\frac{dD}{dt} - \frac{dP}{dt}\right). \tag{4}$$

At a given time t_0, taking Eqs. (1) and (2) into the last equation yields

$$\left.\frac{dV_{FE}}{dt}\right|_{t=t_0} = \frac{d_{FE}}{\varepsilon_0}\left[\frac{V_S}{R} + \frac{2\alpha P_0 + 4\beta P_0^3 + 6\gamma P_0^5}{\rho} - \left(\frac{1}{\rho} + \frac{d_{FE}}{R}\right)E_0\right], \tag{5}$$

where P_0 and E_0 are the polarization and electric field across the ferroelectric at a given time t_0, respectively. Equation (5) indicates that the transient NC depends on not only V_S and R, but also α, β, γ and ρ. The parameters V_S and R are related to the extrinsic characteristics of the R-FEC circuit, while parameters α, β, γ and ρ are the intrinsic parameters of ferroelectric material and determined by the material itself. This means that transient NC depends not only on extrinsic factors in the R-FEC circuit, but also on the ferroelectric material itself. Therefore, it is possible to realize that the change of polarization with time is greater than that of free charge change with time by adjusting the intrinsic parameters α, β, and γ, resulting in the appearance of transient NC.

3.2. Influence of thermodynamic coefficients on transient NC based on experimental measurement

3.2.1. Ferroelectricity

We next characterize electrical properties of the fabricated TiN/HZO/TiN capacitors to discuss the influence of different ratios of hafnium and zirconium on ferroelectricity. The measured *P*–*E* curves of the TiN/HZO/TiN capacitors with the ZrO_2 content of 0.1–0.9 are plotted in Fig. 3. At the low ZrO_2 content of 0.1 in Fig. 3(a), the *P*–*E* curve almost presents the linear distribution, meaning that the sample has the dielectric property. When the ZrO_2 content is changed from 0.25 to 0.5 in Figs. 3(b)–3(d), the *P*–*E* curves present a hysteresis loop, and the hysteresis gradually becomes larger. This mean that these samples have the ferroelectricity, and ferroelectricity enhances with the increase of the ZrO_2 content. At the high ZrO_2 content of 0.6–0.9 in Figs. 3(e)–3(g), the *P*–*E* curves present a double hysteresis loop, which means that the samples have the antiferroelectricity. These results indicate that the sample shows the phase transition from dielectric to ferroelectric to antiferroelectric as the ZrO_2 content increases from 0.1 to 0.9. This can be attributed to the structural phase transition of HZO from monoclinic to orthorhombic to tetragonal phase.[52,53] In addition, in Figs. 3(d) and 3(e), the hysteresis curves are not closed, which is caused by leakage current, charge injection, back injection, and defects of the material itself.

Figure 4 shows the remnant polarization of the HZO thin films as a function of ZrO_2 content. It can be seen that the remnant polarization increases first and then decreases as the ZrO_2 content increases from 0.1 to 0.9, and the sample with the same Hf and Zr contents (sample $Hf_{0.5}Zr_{0.5}O_2$) has the largest remnant polarization of 18 μC/cm^2, which corresponds to the strongest ferroelectricity in Fig. 3(d).

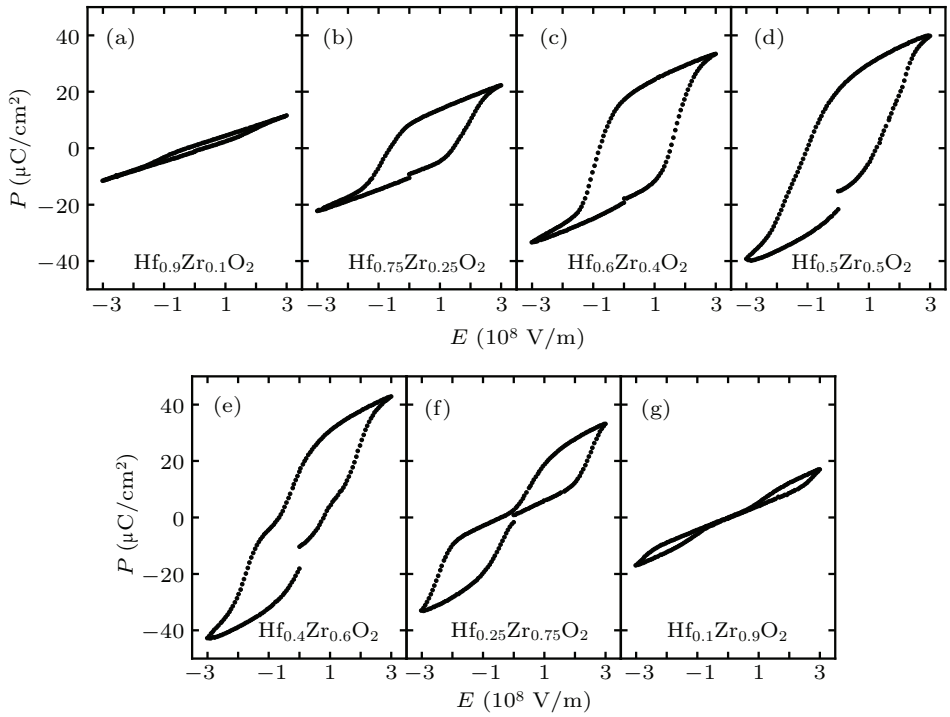


Fig. 3. The *P*–*E* curves of TiN/HZO/TiN capacitors with different ZrO_2 contents.

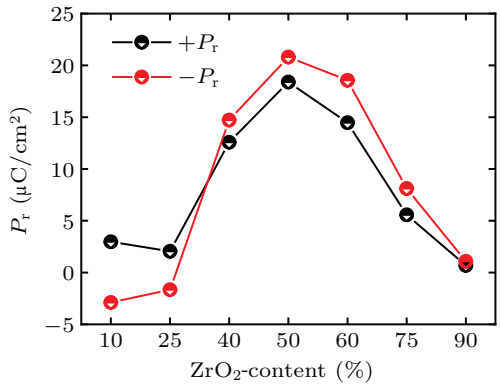


Fig. 4. The remnant polarization of HZO capacitors as a function of ZrO_2 content.

3.2.2. Thermodynamic coefficients

We choose the samples of $Hf_{0.5}Zr_{0.5}O_2$, $Hf_{0.6}Zr_{0.4}O_2$ and $Hf_{0.75}Zr_{0.25}O_2$ with ferroelectricity to investigate the influence of intrinsic ferroelectric parameters on transient NC. Based on the L-G-D theory, the "S"-shaped *P*–*E* curves of these samples are simulated to the corresponding measured *P*–*E* hysteresis loops, as shown in Fig. 5. It can be seen that the simulated S-shaped *P*–*E* curve of sample $Hf_{0.5}Zr_{0.5}O_2$ is similar to that of $Hf_{0.6}Zr_{0.4}O_2$, while they are obviously different from the S-shaped *P*–*E* curve of sample $Hf_{0.75}Zr_{0.25}O_2$. This indicate that the negative slope of the S-shaped *P*–*E* curve for the HZO ferroelectric material is related to ZrO_2 contents.

The thermodynamic coefficients α, β, and γ are further extracted from the simulated S-shaped P–E curves, listed in Table 2. It shows that the coefficients α and β for samples $Hf_{0.5}Zr_{0.5}O_2$ and $Hf_{0.6}Zr_{0.4}O_2$ are similar, which are clearly smaller than that of $Hf_{0.75}Zr_{0.25}O_2$, especially for α. This causes the difference of the S-shaped P–E curves for these samples in Fig. 5. The thermodynamic coefficients γ for these three samples are assumed as zero. These results indicate that the thermodynamic coefficients α and β are related to the ferroelectric material itself.

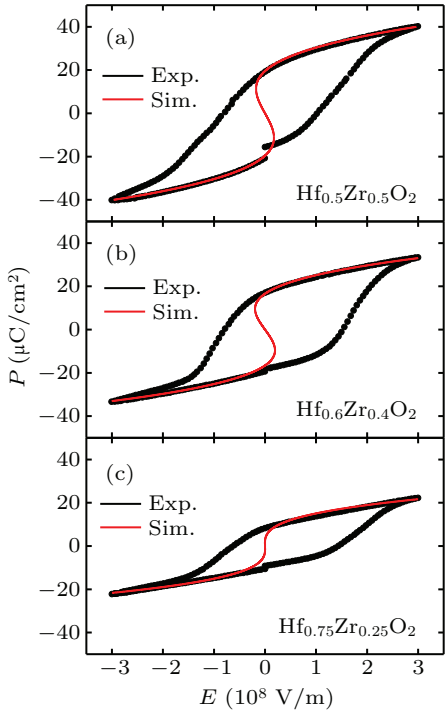


Fig. 5. The measured P–E hysteresis curves (black lines) and the simulated S-shape P–E curves (red lines).

Table 2. The thermodynamic coefficients of HZO capacitors.

Sample	Thermodynamic coefficients		
	α (m/F)	β (m^5/C^{2}F)	γ
$Hf_{0.5}Zr_{0.5}O_2$	-1.1655×10^8	1.5225×10^9	0
$Hf_{0.6}Zr_{0.4}O_2$	-1.529×10^8	2.777×10^9	0
$Hf_{0.75}Zr_{0.25}O_2$	-8.56×10^6	7.467×10^9	0

3.2.3. Transient NC

We finally simulate the transient responses of R-FEC circuit for different ferroelectric HZO capacitors. The input step voltage pulse V_S is -3 V$\rightarrow+3$ V$\rightarrow-3$ V, and the external resistance and the viscosity coefficient are set to 50 kΩ and 500 m·sec/F, respectively. Figure 6 shows the voltage V_{FE} across ferroelectric capacitors as a function of time. It can be seen from Figs. 6(a) and 6(b) that for samples $Hf_{0.5}Zr_{0.5}O_2$ and $Hf_{0.6}Zr_{0.4}O_2$, when the voltage pulse changes from -3 V$\rightarrow+3$ V, as the evolution of time, the V_{FE} increases first, then decreases, then increases again, and finally reaches a stable state. When the voltage pulse changes from $+3$ V$\rightarrow-3$ V, the V_{FE} decreases first, then increases, then decreases again, and finally reaches a stable state. This process is opposite to the case of input voltage pulse of -3 V$\rightarrow+3$ V. We also plot the free charge on metal plates as a function of time in Fig. 6. It shows that with the evolution of time, the free charge increases first and then reaches a stable state under the voltage pulse of -3 V$\rightarrow+3$ V, which is opposite to the change of free charge under $+3$ V$\rightarrow-3$ V. The above results mean that, there are two regions, where with the increase (decrease) of free charge, the voltage across the ferroelectric capacitor decreases (increases), that is, $\mathrm{d}Q/\mathrm{d}V_{FE}<0$. This indicates that transient NC occurs in these two regions.

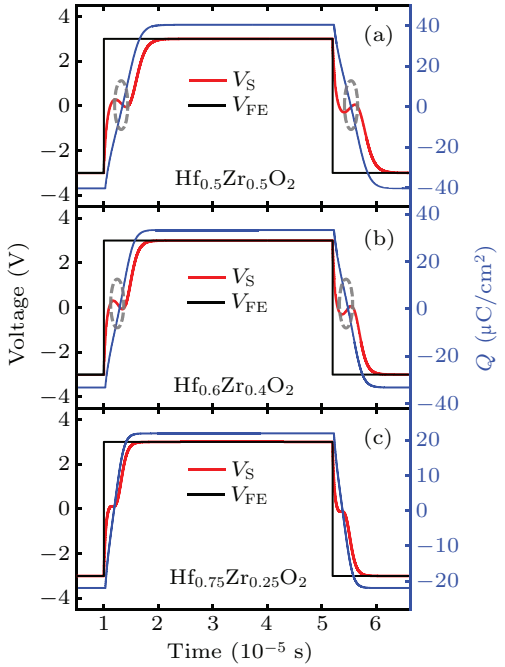


Fig. 6. The input step voltage (black lines), voltage across ferroelectric capacitors (red lines) and free charge on metal plates (blue lines) as a function of time.

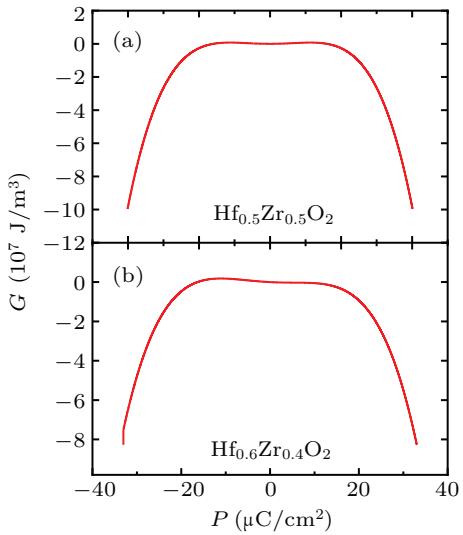


Fig. 7. The Gibbs free energy profiles as a function of polarization P.

For sample $Hf_{0.75}Zr_{0.25}O_2$ in Fig. 6(c), both the V_{FE} and free charge increase (decrease) with the time under voltage pulse, indicating that there is no transient NC phenomenon. This is because the ferroelectricity of sample $Hf_{0.75}Zr_{0.25}O_2$ is significantly weak, and its thermodynamic coefficients α and

β are obviously larger than those of samples $Hf_{0.5}Zr_{0.5}O_2$ and $Hf_{0.6}Zr_{0.4}O_2$, especially for α (sample $Hf_{0.75}Zr_{0.25}O_2$ is one order of magnitude larger than other two samples).

In addition, we simulate the distributions of Gibbs free energy G of samples $Hf_{0.5}Zr_{0.5}O_2$ and $Hf_{0.6}Zr_{0.4}O_2$, as shown in Fig. 7. It can be seen that the distribution of G presents the "M" shape. As the polarization increases, G first increases, then decreases, then increases, and finally decreases. This indicates that the thermodynamic process of transient NC does not follow the generally accepted viewpoint of the minimization of G.

4. Conclusion

The influence of thermodynamic coefficients on transient NC for Zr-doped HfO_2 thin film is systemically investigated. Our results show that the HZO thin film undergoes the ferroelectric phase transition from dielectric to ferroelectric to antiferroelectric under the induction of different ZrO_2 contents. Moreover, we find that transient NC effect depends not only on series resistor and viscosity coefficients, but also on thermodynamic coefficients α, β and γ. The smaller coefficients α and β, the more significant the transient NC effect. In addition, we also find the the well known Gibbs free energy minimization is not applicable to understand the thermodynamic process of the transient NC. This work provides a comprehensive understanding of the affect factors on transient NC in the ferroelectric capacitors.

References

[1] Moore G E 1998 *Proc. IEEE* **86** 82
[2] He G, Liu J, Chen H, Liu Y, Sun Z, Chen X, Liu M and Zhang L 2014 *J. Mater. Chem. C* **2** 5299
[3] Gao J, He G, Xiao D, Jin P, Jiang S, Li W, Liang S and Zhu L 2017 *J. Mater. Sci. Technol.* **33** 901
[4] He G, Sun Z, Li G and Zhang L 2012 *Crit. Rev. Solid State Mater. Sci.* **37** 131
[5] Hoffmann M, Slesazeck S, Schroeder U and Mikolajick T 2020 *Nat. Electron.* **3** 504
[6] Li W S, Zhou J, Wang H C, Wang S X, Yu Z H, Li S L, Shi Y and Wang X R 2017 *Acta Phys. Sin.* **66** 218503 (in Chinese)
[7] Zhang N, Xu K K, Chen Y X, Zhu K F, Zhao J M and Yu Q Y 2019 *Acta Phys. Sin.* **68** 167803 (in Chinese)
[8] Xu X X, Luo Q, Gong T C, Lv H B, Liu Q and Liu M 2021 *Chin. Phys. B* **30** 058702
[9] Theis T N and Solomon P M 2010 *Science* **327** 1600
[10] Zhirnov V V and Cavin R K 2008 *Nat. Nanotechnol.* **3** 77
[11] Salahuddin S and Dattat S 2008 *Nano Lett.* **8** 405
[12] Salvatore G A, Bouvet D and Ionescu A M 2008 *Proceedings of the 54th IEEE International Electron Devices Meeting (IEDM)*, December 3–7, 2008, San Francisco, America, p. 1
[13] Jain A and Alam M A 2014 *IEEE Trans. Electron Devices* **61** 2235
[14] McGuire F A, Cheng Z, Price K and Franklin A D 2016 *Appl. Phys. Lett.* **109** 093101
[15] Yuan Z C, Rizwan S, Wong M, Holland K, Anderson S, Hook T B, Kienle D, Gadelrab S, Gudem P S and Vaidyanathan M 2016 *IEEE Trans. Electron Devices* **63** 4046
[16] Zhou J, Han G, Li Q, Peng Y, Lu X, Zhang C, Zhang J, Sun Q Q, Zhang D W and Hao Y 2016 *Proceedings of the 62th IEEE International Electron Devices Meeting (IEDM)*, December 3–7, 2016, San Francisco, America, p. 12.2. 1
[17] Zhou J, Wu J, Han G, Kanyang R, Peng Y, Li J, Wang H, Liu Y, Zhang J and Sun Q Q 2017 *Proceedings of the 63th IEEE International Electron Devices Meeting (IEDM)*, December 1–5, 2017, San Francisco, America, p. 15.5. 1
[18] Lee M, Chen K T, Liao C Y, Gu S S, Siang G Y, Chou Y C, Chen H Y, Le J, Hong R C and Wang Z Y 2018 *Proceedings of the 64th IEEE International Electron Devices Meeting (IEDM)*, December 2–6, 2018, San Francisco, America, p. 31.8. 1
[19] Si M, Su C J, Jiang C, Conrad N J, Zhou H, Maize K D, Qiu G, Wu C T, Shakouri A and Alam M A 2018 *Nat. Nanotechnol.* **13** 24
[20] Alam M A, Si M and Ye P D 2019 *Appl. Phys. Lett.* **114** 090401
[21] Chen J D, Han W H, Yang C, Zhao X S, Guo Y Y, Zhang X Di and Yang F H 2020 *Acta Phys. Sin.* **69** 137701 (in Chinese)
[22] Khan A I, Keshavarzi A and Datta S 2020 *Nat. Electron.* **3** 588
[23] Li K S, Chen P G, Lai T Y, Lin C H, Cheng C C, Chen C C, Wei Y J, Hou Y F, Liao M H and Lee M H 2015 *Proceedings of the 61th IEEE International Electron Devices Meeting (IEDM)*, December 5–9, 2015, San Francisco, America, p. 22.6. 1
[24] Kwon D, Chatterjee K, Tan A J, Yadav A K, Zhou H, Sachid A B, Dos Reis R, Hu C and Salahuddin S 2017 *IEEE Electron Device Lett.* **39** 300
[25] Zubko P, Wojdeł J C, Hadjimichael M, Fernandez-Pena S, Sené A, Luk'yanchuk I, Triscone J M and Íñiguez J 2016 *Nature* **534** 524
[26] Yadav A K, Nguyen K X, Hong Z, García-Fernández P, Aguado-Puente P, Nelson C T, Das S, Prasad B, Kwon D and Cheema S 2019 *Nature* **565** 468
[27] Khan A I, Chatterjee K, Wang B, Drapcho S, You L, Serrao C, Bakaul S R, Ramesh R and Salahuddin S 2015 *Nat. Mater.* **14** 182
[28] Hoffmann M, Pešić M, Chatterjee K, Khan A I, Salahuddin S, Slesazeck S, Schroeder U and Mikolajick T 2016 *Adv. Funct. Mater.* **26** 8643
[29] Kobayashi M, Ueyama N, Jang K and Hiramoto T 2016 *Proceedings of the 62th IEEE International Electron Devices Meeting (IEDM)*, December 3–7, 2016, San Francisco, America, p. 12.3. 1
[30] Kim Y J, Park H W, Hyun S D, Kim H J, Kim K D, Lee Y H, Moon T, Lee Y B, Park M H and Hwang C S 2017 *Nano Lett.* **17** 7796
[31] Sharma P, Zhang J, Ni K and Datta S 2017 *IEEE Electron Device Lett.* **39** 272
[32] Jang K, Ueyama N, Kobayashi M and Hiramoto T 2018 *IEEE J. Electron Devices Society* **6** 346
[33] Hoffmann M, Slesazeck S and Mikolajick T 2021 *APL Mater.* **9** 020902
[34] Khan A I, Bhowmik D, Yu P, Joo Kim S, Pan X, Ramesh R and Salahuddin S 2011 *Appl. Phys. Lett.* **99** 113501
[35] Appleby D J, Ponon N K, Kwa K S, Zou B, Petrov P K, Wang T, Alford N M and O'Neill A 2014 *Nano Lett.* **14** 3864
[36] Gao W, Khan A, Marti X, Nelson C, Serrao C, Ravichandran J, Ramesh R and Salahuddin S 2014 *Nano Lett.* **14** 5814
[37] Wang Z, Li H, Hu H, Fan Y, Fan R, Li B, Zhang J, Liu H, Fan J and Hou H 2020 *Adv. Electron. Mater.* **6** 1901005
[38] Kittl J, Obradovic B, Reddy D, Rakshit T, Hatcher R and Rodder M 2018 *Appl. Phys. Lett.* **113** 042904
[39] Liu Z, Bhuiyan M and Ma T 2018 *Proceedings of the 64th IEEE International Electron Devices Meeting (IEDM)*, December 2–6, 2018, San Francisco, America, p. 31.2. 1
[40] Van Houdt J and Roussel P 2018 *IEEE Electron Device Lett.* **39** 877
[41] Landau L D and Lifshitz E M 1960 *Electrodynamics of Continuous Media* (Pergamon, Oxford)
[42] Landau L D 1937 *Zh. Eksp. Teor. Fiz.* **7** 19
[43] Ginzburg V L 1945 *Zh. Eksp. Teor. Fiz* **15** 739
[44] Devonshire A F 1949 *Phil. Mag.* **40** 1040
[45] Chang S C, Avci U E, Nikonov D E, Manipatruni S and Young I A 2018 *Phys. Rev. Appl.* **9** 014010
[46] Song S J, Kim Y J, Park M H, Lee Y H, Kim H J, Moon T, Do Kim K, Choi J H, Chen Z, Jiang A and Hwang C S 2016 *Sci. Rep.* **6** 20825
[47] Saha A K, Datta S and Gupta S K 2018 *J. Appl. Phys.* **123** 105102
[48] Zhang Y, Ma X, Wang X, Han K, Xiang J and Wang W 2020 *J. Phys. D: Appl. Phys.* **53** 455106
[49] Li Y, Wang Y, Lu W, Kong X, Han L and Zhao H 2020 *Chin. Phys. B* **30** 050703
[50] Ricinschi D, Harnagea C, Papusoi C, Mitoseriu L, Tura V and Okuyama M 1998 *J. Phys. Condens. Matter* **10** 477
[51] Jiang S, He G, Liu M, Zhu L, Liang S, Li W, Sun Z and Tian M 2018 *Adv. Electron. Mater.* **4** 1700543
[52] Muller J, Böscke T S, Schröder U, Mueller S, Brauhaus D, Bottger U, Frey L and Mikolajick T 2012 *Nano Lett.* **12** 4318
[53] Zhou Z, Wang J, Chen J, Jiang C, Li L and Liu M 2021 *J. Mater. Chem. C* **9** 649